

A Rare and Highly Oxidized Mo₂^{5.5+} Unit Stabilized by Oxo Anions and Supported by Formamidinate Bridges

F. Albert Cotton,* Carlos A. Murillo,* Rongmin Yu, and Qinliang Zhao

Department of Chemistry and Laboratory for Molecular Structure and Bonding, P.O. Box 3012, Texas A&M University, College Station, Texas 77842-3012

Received July 20, 2006

A series of tetranuclear compounds consisting of two {Mo₂[(*m*-CF₃C₆H₄)NC(H)N(*m*-CF₃C₆H₄)₃]}ⁿ⁺ moieties linked by two OH⁻ or two O²⁻ ions has been characterized. Abbreviating the dimolybdenum plus three spectator bridging ligands as [Mo₂], the following three compounds have been made—[Mo₂](μ-OH)₂[Mo₂] (**1**), [Mo₂](μ-O)₂[Mo₂] (**2**), and {[Mo₂](μ-O)₂[Mo₂]}SbF₆ (**3**). Compound **1**, which is diamagnetic and contains quadruply bonded Mo₂⁴⁺ units, is converted to diamagnetic **2** by oxidation with O₂. Compound **2**, which has Mo₂⁵⁺ units, is oxidized by NOSbF₆ to **3** which has a rare Mo₂^{5.5+} core and an odd electron delocalized over the two dimolybdenum units.

Introduction

Mixed-valence compounds (MVCs) have been of great interest for decades because of their fundamental importance in understanding many important chemical and biological processes.¹ Most of the studies in this area have focused on systems with single-metal redox centers, generically M–L–M species, which resemble the well-known Creutz–Taube complex.² However, the range has now been extended to dinuclear systems, M₂–L–M₂.³ In this laboratory, we have found that MVCs having Mo₂(DAniF)₃⁺ with a quadruply bonded dimolybdenum unit and Mo₂(DAniF)₃²⁺ (Mo₂⁵⁺) units can be prepared readily from molecular pairs with two identical Mo₂(DAniF)₃⁺ units (DAniF = *N,N'*-di-*p*-anisyl-formamidinate).⁴ An important advantage in having redox centers with Mo₂ units is that their electronic structures and molecular structures are well established.⁵ The change of the electron number in the metal orbitals can be tracked

unambiguously in the Mo–Mo distances, and thus, the distribution of the odd electron in the MVCs, especially for the localized system, can be determined or estimated from the single-crystal structures.^{4c}

The chemistry of quadruply bonded dimolybdenum compounds with formamidinate ligands has been investigated

* To whom correspondence should be addressed. E-mail: cotton@tamu.edu (F.A.C.); murillo@tamu.edu (C.A.M.).

(1) See for example: (a) Prassides, K., Ed. *Mixed-valency Systems: Applications in Chemistry, Physics and Biology*; Kluwer Academic Publishers: Dordrecht, 1991. (b) Cembran, A.; Bernardi, F.; Olivucci, M.; Garavelli, M. *Proc. Nat. Acad. Sci. U.S.A.* **2005**, *102*, 6255. (c) Talukdar, P.; Bollot, G.; Mareda, J.; Sakai, N.; Matile, S. *J. Am. Chem. Soc.* **2005**, *127*, 6528. (d) Fiedler, A. T.; Bryngelson, P. A.; Maroney, M. J.; Brunold, T. C. *J. Am. Chem. Soc.* **2005**, *127*, 5449. (e) Sakharov, D. V.; Lim, C. *J. Am. Chem. Soc.* **2005**, *127*, 4921. (f) Efimov, I.; McIntire, W. S. *J. Am. Chem. Soc.* **2005**, *127*, 732. (g) O'Neill, M. A.; Dohno, C.; Barton, J. K. *J. Am. Chem. Soc.* **2004**, *126*, 1316. (h) Lewis, F. D.; Wu, Y.; Zhang, L.; Zuo, X.; Gayes, R. T.; Wasielewski, M. R. *J. Am. Chem. Soc.* **2004**, *126*, 8206. (i) Wan, C.; Fiebig, T.; Schiemann, O.; Barton, J. K.; Zewail, A. H. *Proc. Nat. Acad. Sci. U.S.A.* **2000**, *97*, 14052. (j) Hess, S.; Götz, M.; Davis, W. B.; Michel-Beyerle, M. E. *J. Am. Chem. Soc.* **2001**, *123*, 10046.

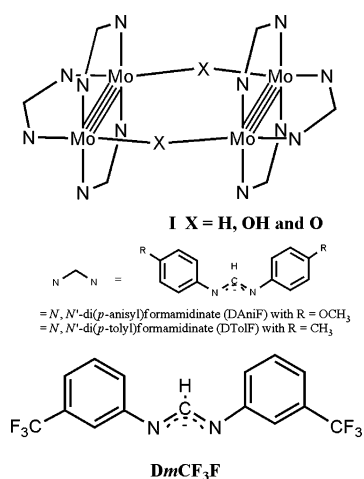
(2) (a) Creutz, C.; Taube, H. *J. Am. Chem. Soc.* **1969**, *91*, 3988. (b) Creutz, C.; Taube, H. *J. Am. Chem. Soc.* **1973**, *95*, 1086. (c) Creutz, C. *Prog. Inorg. Chem.* **1983**, *30*, 1. (d) Richardson, D. E.; Taube, H. *Coord. Chem. Rev.* **1984**, *60*, 107. (e) Dogan, A.; Sarkar, B.; Klein, A.; Lissner, F.; Schleid, T.; Fiedler, J.; Zalis, S.; Jain, V. K.; Kaim, W. *Inorg. Chem.* **2004**, *43*, 5973. (f) Rigaut, S.; Olivier, C.; Costuas, K.; Choua, S.; Fadhel, O.; Massue, J.; Turek, P.; Saillard, J. Y.; Dixneuf, P. H.; Touchard, D. *J. Am. Chem. Soc.* **2006**, *128*, 5859. (g) D'Alessandro, D. M.; Dinolfo, P. H.; Davies, M. S.; Hupp, J. T.; Keene, F. R. *Inorg. Chem.* **2006**, *45*, 3261. (h) Crutchley, R. J. *Adv. Inorg. Chem.* **1994**, *41*, 273. (i) Kaim, W.; Klein, A.; Glöckle, M. *Acc. Chem. Res.* **2000**, *33*, 755. (j) Demadis, K. D.; Harshorn, M.; Meyer, T. J. *Chem. Rev.* **2001**, *101*, 2655.

(3) (a) Cotton, F. A.; Lin, C.; Murillo, C. A. *Acc. Chem. Res.* **2001**, *34*, 759. (b) Chisholm, M. H.; Macintosh, A. M. *Chem. Rev.* **2005**, *105*, 2949.

(4) (a) Cotton, F. A.; Donahue, J. P.; Murillo, C. A. *Inorg. Chem.* **2001**, *40*, 2229. (b) Cotton, F. A.; Liu, C. Y.; Murillo, C. A.; Wang, X. *Inorg. Chem.* **2003**, *42*, 4619. (c) Cotton, F. A.; Dalal, N. S.; Liu, C. Y.; Murillo, C. A.; North, J. M.; Wang, X. *J. Am. Chem. Soc.* **2003**, *125*, 12945. (d) Cotton, F. A.; Donahue, J. P.; Lin, C.; Murillo, C. A. *Inorg. Chem.* **2001**, *40*, 1234. (e) Cotton, F. A.; Donahue, J. P.; Murillo, C. A. *J. Am. Chem. Soc.* **2003**, *125*, 5436. (f) Cotton, F. A.; Donahue, J. P.; Murillo, C. A.; Pérez, L. M. *J. Am. Chem. Soc.* **2003**, *125*, 5486. (g) Cotton, F. A.; Daniels, L. M.; Donahue, J. P.; Liu, C. Y.; Murillo, C. A. *Inorg. Chem.* **2002**, *41*, 1354. (h) Cotton, F. A.; Liu, C. Y.; Murillo, C. A.; Villagrán, D.; Wang, X. *J. Am. Chem. Soc.* **2003**, *125*, 13564. (i) Cotton, F. A.; Liu, C. Y.; Murillo, C. A.; Villagrán, D.; Wang, X. *J. Am. Chem. Soc.* **2004**, *126*, 14822. (j) Cotton, F. A.; Donahue, J. P.; Murillo, C. A.; Pérez, L. M.; Yu, R. *J. Am. Chem. Soc.* **2003**, *125*, 8900.

(5) Cotton, F. A.; Murillo, C. A.; Walton, R. A. *Multiple Bonds Between Metal Atoms*; Springer Science and Business Media, Inc.: New York, 2005.

Scheme 1



extensively,⁵ and an important series of 10 dimolybdenum paddlewheel compounds with such ligands was prepared and investigated structurally and electrochemically by Ren and co-workers.⁶ The aryl groups in the formamidinate ligands ranged from those having strongly donating groups such as anisyl groups to those with electron withdrawing species such as *m*-, *p*-CF₃C₆H₄, and 3,5-Cl₂C₆H₃ groups. All those compounds show only one metal-based redox process (i.e., Mo₂⁴⁺/Mo₂⁵⁺). Indeed further oxidations of Mo₂-(formamidinate)₄ have never been documented. In fact, dimolybdenum compounds with a 6+ core charge are so uncommon that the only known species are paddlewheel compounds with guanidinate ligands such as hpp or highly charged anions such as phosphonates and SO₄²⁻.⁵

Previous work in this laboratory⁷ has led to compounds of the general class shown in Scheme 1, in which the bridges, X, have been H, OH, and O. For H-bridged compounds, the formamidinate ligands (DArF) have been those with Ar = *N-p*-tolyl (Tol) and *N-p*-anisyl (Ani) groups, and the singly oxidized compounds with [Mo₂(DArF)₃(μ-H)₂Mo₂(DArF)₃]⁺ ions have also been prepared and studied.⁸ For the μ-OH and μ-O compounds, only those with DTolF as ancillary ligands have been reported.⁷

In this report, we describe further studies of the μ-OH- and μ-O-type compounds in which the ancillary ligands are di-*m*-CF₃-phenylformamidinate, which we shall abbreviate as DmCF₃F, shown at the bottom of Scheme 1. This ligand, which is easy to make and handle and also affords crystalline products that have good solubility properties, is less basic than the DAniF ligand that we have so extensively employed in the past.⁴

Results and Discussion

Syntheses and Structural Results. The compound Mo₂-(DmCF₃F)₃(μ-OH)₂Mo₂(DmCF₃F)₃ (**1**) was prepared readily

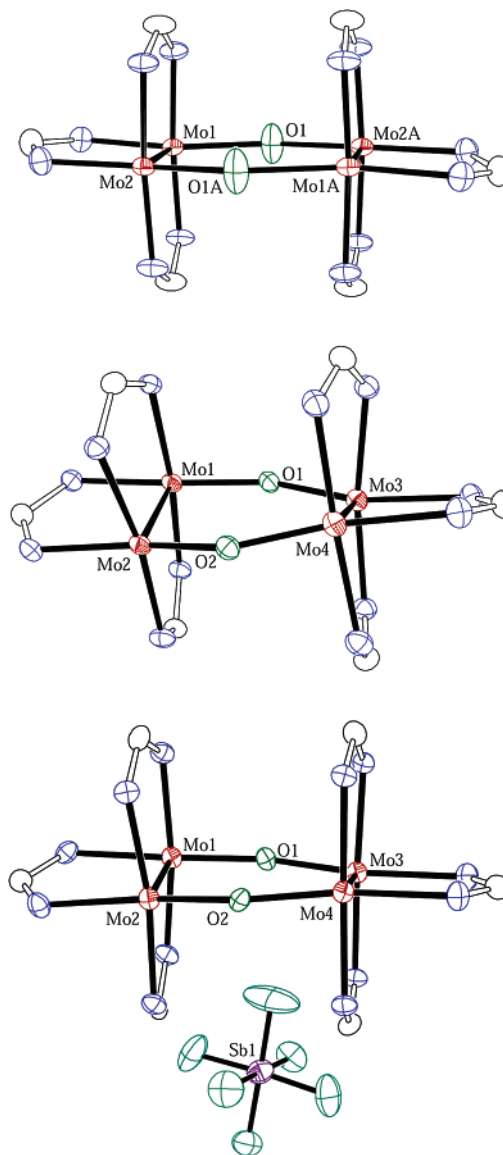


Figure 1. Core structures of **1**·CH₂Cl₂ (top), **2**·H₂O (center), and **3**·H₂O·CH₂Cl₂ (down) drawn with ellipsoids at the 40% probability level. All *m*-CF₃C₆H₄ groups and hydrogen atoms have been omitted for clarity.

from Mo₂(OAc)₄ via a two-step reaction in which Mo₂(OAc)₄ was mixed with 3 equiv of the formamidine followed by the addition of sodium methoxide. This preparation is much easier to control than that reported for the analogous compound [Mo₂(DTolF)₃]₂(μ-OH)₂ which was synthesized by reacting Mo₂(DTolF)₃Cl₂ and K/Hg in the presence of moisture.^{7b}

The structural analysis revealed that **1** is composed of two Mo₂(DmCF₃F)₃⁺ units linked by two OH bridging groups, as shown in Figure 1. The Mo₂ units have the typical eclipsed conformation for dimolybdenum compounds with quadruple bonds.⁵ The compound crystallizes in the triclinic space group *P* $\bar{1}$ with *Z* = 1 in which the tetranuclear molecule resides on a crystallographic inversion center. The molybdenum atoms and the bridging oxygen atoms from the hydroxide groups form an essentially flat six-membered ring. The Mo–Mo distances of 2.1004(6) Å (Table 1) are in the typical range for a quadruply bonded Mo₂⁴⁺ unit with an electronic configuration of σ²π⁴δ².⁵ The independent Mo–O

(6) Lin, C.; Protasiewicz, J. D.; Ren, T. *Inorg. Chem.* **1996**, *35*, 6422.

(7) (a) Cotton, F. A.; Daniels, L. M.; Jordan IV, G. T.; Lin, C.; Murillo, C. A. *J. Am. Chem. Soc.* **1998**, *120*, 3398. (b) Cotton, F. A.; Daniels, L. M.; Guimet, I.; Henning, R. W.; Jordan, G. T.; Lin, C.; Murillo, C. A.; Schultz, A. J. *J. Am. Chem. Soc.* **1998**, *120*, 12531. (c) Cotton, F. A.; Daniels, L. M.; Jordan IV, G. T.; Lin, C.; Murillo, C. A. *Inorg. Chem. Commun.* **1998**, 109.

(8) Cotton, F. A.; Donahue, J. P.; Huang, P.; Murillo, C. A.; Villagrán, D. *Z. Anorg. Allg. Chem.* **2005**, *631*, 2606.

Table 1. Selected Bond Distances (Å) and Angles (deg)

	1 ·CH ₂ Cl ₂	2 ·H ₂ O	3 ·H ₂ O·CH ₂ Cl ₂
Mo(1)–Mo(2)	2.1004(6)	2.1526(6)	2.161(1)
Mo(3)–Mo(4)		2.1516(6)	2.172(1)
Mo ₂ ···Mo ₂ ^a	4.082	3.690	3.699
Mo(1)–O(1)	2.136(3)	1.937(2)	1.944(4)
Mo(2)–O(2)		1.927(2)	1.926(4)
Mo(3)–O(1)	2.132(3) ^b	1.922(2)	1.892(4)
Mo(4)–O(2)		1.927(2)	1.898(4)
Mo–O(1)–Mo	146.0(1)	148.2(1)	151.4(3)
Mo–O(2)–Mo		148.7(1)	150.0(3)
Mo–N (av.)	2.142[3]	2.171[3]	2.150[5]

^a Distances between the midpoints of the two [Mo₂] units. ^b Mo(2A)–O(1).

distances of 2.136(3) and 2.132(3) Å are long and consistent with the bridging groups being OH[−] rather than O^{2−}. This assignment is further supported by the presence of a signal for the OH group at 2.693 ppm in the ¹H NMR spectrum measured in CDCl₃.

Compound **2**, whose structure is also shown in Figure 1, was synthesized by air oxidation of solutions of **1**. It should be noted that **1** is moderately air-sensitive even in the solid state, and its yellow solutions quickly turn green when exposed to air. Once oxidation takes place, the product appears to be relatively stable in solution and very stable in the solid state.⁹ If an intermediate singly oxidized species is produced when **1** is oxidized to **2**, it has not been detected in either CH₂Cl₂ solution or in the solid state.^{10,11} Compound **2** is composed of two Mo₂(DmCF₃F)₃²⁺ units linked by two oxide bridges in which each Mo₂⁵⁺ unit has a nominal electronic configuration of $\sigma^2\pi^4\delta$ which results in paramagnetic species in dinuclear compounds.⁵ However, **2** is diamagnetic, as shown by its NMR spectrum. The diamagnetism indicates that there is strong antiferromagnetic coupling between the dimolybdenum units mediated by the linking oxo groups.

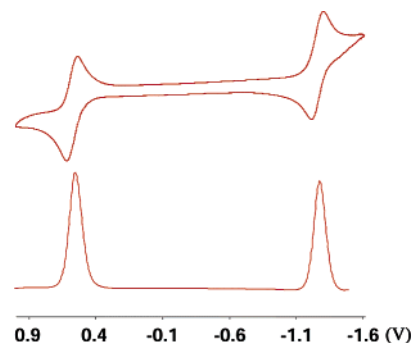
The dimolybdenum units in **2** show a slightly staggered conformation instead of the eclipsed one in **1**. The average torsion angle of N–Mo–Mo–N is 7.5[1]°. Because of the staggered conformation, the six-membered ring of the molybdenum atoms and the bridging oxygen atoms is not planar. The torsion angles of O1–Mo1–Mo2–O2 and O1–Mo3–Mo4–O2 are 17.49(9)° and 18.77(9)°, respectively. The crystallographically independent distances of Mo–Mo bonds, 2.1526(6) and 2.1516(6) Å, are about 0.05 Å longer than those in compound **1**. The lengthening of the Mo–Mo bond by about 0.04–0.05 Å is typically found in one-electron oxidations of Mo₂⁴⁺ units.^{4c,12} Clearly, one electron has been removed from a δ bonding orbital in each Mo₂(DmCF₃F)₃ unit after oxidation. Therefore, the bond order between Mo

(9) No changes were observed in the ¹H NMR of **2** upon exposure to air for a few hours, but changes were noted after 24 h. For the crystalline samples, no changes were observed when samples were stored in air for over a month.

(10) Efforts to detect such an intermediate by EPR spectroscopy gave no positive result.

(11) It should also be noted that the fate of the hydrogen atoms from the μ -OH groups was not determined, but recent work on a similar system suggest that they are lost as H₂O.

(12) Cotton, F. A.; Daniels, L. M.; Hillard, E. A.; Murillo, C. A. *Inorg. Chem.* **2002**, *41*, 1639.

**Figure 2.** Cyclic voltammogram (CV) and differential potential voltammogram (DPV) of **2** in CH₂Cl₂. All potentials are referenced to Ag/AgCl.

atoms is 3.5 in each dimolybdenum units. The identity of the bridging group is O^{2−} rather than OH[−] is supported by two facts: the Mo–O bond distances (~1.93 Å) are about 0.2 Å shorter than those in **1** and the proton signal for OH observed in the ¹H NMR spectrum of **1** is absent in the spectrum of **2**.

Compound **3**, the only known example of a MVC with Mo₂^{5.5+} units having dimolybdenum units supported by formamidinate ligands, was prepared from the reaction of **2** and NOSbF₆. This complex is only slightly soluble in CH₂Cl₂, but it is soluble in acetone. The crystals, obtained directly by allowing the reaction mixture to stand undisturbed, belong to the triclinic space group *P* $\bar{1}$ and have *Z* = 2. Compared to its precursor **2**, the overall structure of the cation in **3** is less distorted. The torsion angles of O1–Mo1–Mo2–O2 and O1–Mo3–Mo4–O2 in **3** are 8.2(2)° and 11.6(2)°, respectively. The two crystallographically independent Mo–Mo bond distances are essentially the same (2.161(1) and 2.172(1) Å) but about 0.015 Å longer than those in its precursor, which is consistent with the removal of one electron from a δ bonding orbital. Consequently, only one electron remains in the δ bonding orbitals. The two dimolybdenum units in this compound are structurally equivalent, and the molecule is symmetrical in structure, which is consistent with the delocalization of the unpaired electron over the six-membered (Mo₂)₂O₂ unit, and a formal bond order of 3.25 can be assigned to each of the two electronically equivalent dimolybdenum units.

Electrochemistry. The electrochemistry of **2** in the window from −1.5 to 1.0 V is unique and very interesting, as shown in Figure 2. In CH₂Cl₂ solution, there are two well-separated reversible redox processes with *E*_{1/2} at −1.257 and 0.577 V. The process at −1.257 V corresponds to a reduction to a Mo₂⁴⁺–Mo₂⁵⁺ species,¹³ while that at 0.577 V corresponds to an oxidation to an (Mo₂⁵⁺–Mo₂⁵⁺/Mo₂⁵⁺–Mo₂⁶⁺) species. The latter assignment is supported by the isolation of **3**, having an Mo₂^{5.5+} unit, from the reaction of **2** and 1 equiv of NOSbF₆.

A comparison of the redox potentials of **2** and that of the corresponding paddlewheel compound, Mo₂(DmCF₃F)₄, which has been reported to have an oxidation process at 0.76 V vs Ag/AgCl in CH₂Cl₂,⁶ shows that the first redox potential of

(13) Because this process is reversible, we believe that this species, which has not been isolated, has a dioxo-bridged unit.

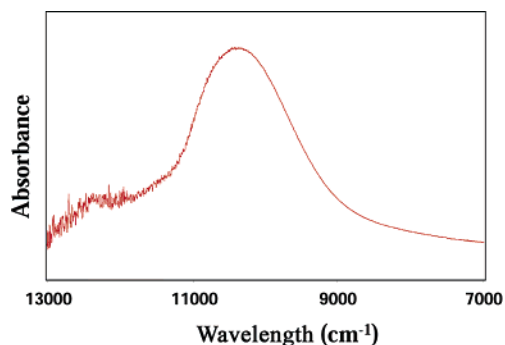


Figure 3. Near-IR spectrum of the crystalline mixed-valence species **3** in KBr pellets.

Table 2. Calculated Bond Lengths (Å) and Angles (deg) for Models of **1**, **2**, and **3**

spin	energy (au)	Mo–Mo	Mo ₂ ···Mo ₂	Mo–O (av)	Mo–N (av)	Mo–O–Mo
1 0	–1318.572	2.155	4.151	2.193	2.133	142.33
2 0	–1317.370	2.194	3.750	1.947	2.164	148.60
1	–1317.345	2.210	3.750	1.974	2.164	143.38
3 1/2	–1317.201	2.210	3.740	1.944	2.151	148.32

2 (–1.257 V), which involves an Mo₂^{5.5+} unit, is displaced by about 2 V. This indicates that the O^{2–} dianion strongly stabilizes higher oxidation states. Interestingly, the hydroxo-bridged analogue **1** shows a cyclic voltammogram (CV) with only one irreversible oxidation process at ca. 0.6 V.¹⁴

Magnetism and NIR Spectra. Both **1** and **2** are diamagnetic, but **3** is paramagnetic. The X-band EPR spectrum for the latter was measured at room temperature in the solid state. Only one prominent signal was observed, which is consistent with a doublet electronic ground state. The *g* value of 1.942 is significantly different from that of an organic free radical and indicates that the unpaired electron resides in a mainly metal-based orbital. The main peak is due to molecules containing the ⁹⁶Mo (*I* = 0) isotope (about 74% abundance). This result is consistent with DFT calculations (vide infra) which show that the SOMO is a metal-based orbital.

The NIR spectrum of **3**, shown in Figure 3, was measured in the solid state using KBr pellets in the region from 2000 to 12 000 cm^{–1}. The mixed-valence complex shows one intense broad absorption band centered at ca. 10 400 cm^{–1} with bandwidth of 1100 cm^{–1} at half-height. This spectrum resembles the NIR spectra of the [Mo₂]L[Mo₂] systems, for which one band has been observed in this region.¹⁵ The intense bands suggest significant electronic interaction between the two dimolybdenum units.

Electronic Structures and DFT Calculations. A series of DFT calculations were carried out to better understand the electronic interaction between the [Mo₂] units. Geometry optimizations for the neutral and singly oxidized species were done using the parameters from the crystal structures as starting points. The models, with all *m*-CF₃ aryl groups

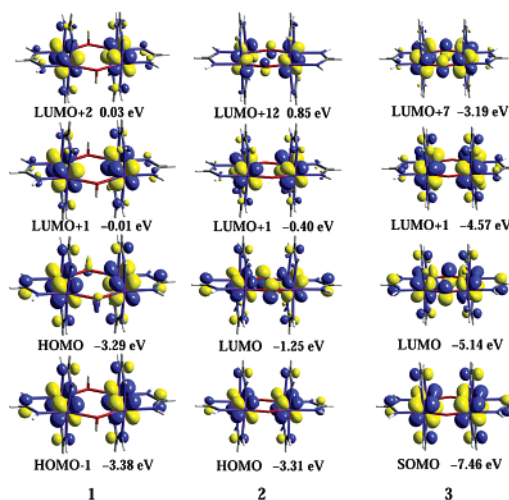


Figure 4. Selected frontier orbitals for the models for **1**, **2** at singlet state, and **3** using an isosurface value of 0.03.

replaced by hydrogen atoms, were simplified to [Mo₂–(NHCHNH)₃]₂(μ-X)₂ (X = O, OH) with C_i symmetry. To gain insight into the electronic transitions responsible for the observed electronic spectra, time-dependent density functional theory (TD-DFT) calculations¹⁶ were performed using the Gaussian program suite.

The general agreement between the calculated and the experimental geometric data shown in Tables 1 and 2 suggests that such a simplification is reasonable. The overestimation of the Mo–Mo distances (ca. 0.05 Å) is reasonable because of the use of hydrogen atoms instead of the electron-withdrawing *m*-CF₃C₆H₅ groups. All changes in bond distances and angles resulting from the oxidation are in good agreement with those from X-ray crystallography. Upon oxidation of **1** to **2**, the calculated distances between the midpoints of the two [Mo₂] units decreased by about 0.40 Å, while the Mo–Mo distances increased by 0.05 Å; these changes are comparable with the experimental variations which are ca. 0.39 and 0.04 Å, respectively. The changes in Mo–Mo distances upon oxidation of **2** were also consistent with those obtained from the DFT calculation.

The diamagnetism of **2** suggests that the singlet state should be more stable than the triplet state. The calculations indeed showed that the singlet state is favored by 15.7 kcal mol^{–1}. As shown in Table 2, the optimized geometry of the singlet state resulted in better agreement with the experimental values in Table 1. The very large HOMO/LUMO gap of 2.06 eV (47.5 kcal mol^{–1}) accounts for the observed diamagnetism (Figure 4), and supports the existence of strong antiferromagnetic coupling between the dimolybdenum units in **2**.

Analysis of the frontier orbitals from the calculations (Figure 4) indicates that the p orbitals from the hydroxide and oxide bridges contribute to the electronic communication between the two dimetal units. Because of the strong interaction with the p orbitals from the linker, the δ orbitals

(14) Irreversible oxidation processes are not uncommon in systems with OH groups.

(15) (a) Cotton, F. A.; Li, Z.; Liu, C. Y.; Murillo, C. A.; Villagrán, D. *Inorg. Chem.* **2006**, *45*, 767. (b) Cotton, F. A.; Murillo, C. A.; Villagrán, D.; Yu, R. *J. Am. Chem. Soc.* **2006**, *128*, 3281. (c) Chisholm, M. H.; Pate, B. D.; Wilson, P. J.; Zalesky, J. M. *Chem. Commun.* **2002**, 1084.

(16) Casida, M. E.; Jamorski, C.; Casida, K. C.; Salahub, D. R. *J. Chem. Phys.* **1998**, *108*, 4439.

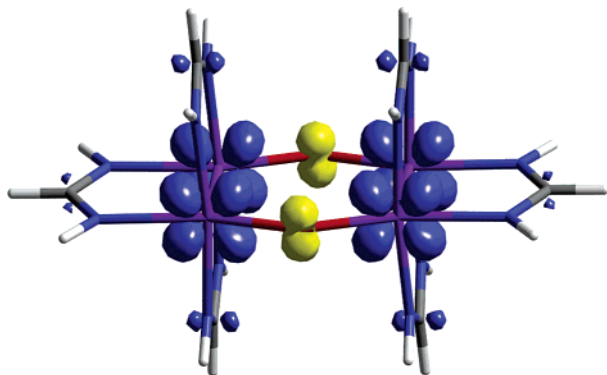


Figure 5. Spin density diagram of the SOMO in models for **3** with a 0.006 isosurface value.

from the two dimetal units generate two molecular orbitals, one out-of-phase ($\delta - \delta$) and one in-phase ($\delta + \delta$) combination of the δ orbitals. The two δ^* orbitals gives two more molecular orbitals, which again include one out-of-phase ($\delta^* - \delta^*$) and one in-phase ($b_{2u}, \delta^* + \delta^*$) combination with different orbital energies.

The DFT calculations on **3** also provide information on the way the unpaired electron is distributed in the cation. The spin density diagram of the SOMO (Figure 5) shows that the odd electron is delocalized over the two dimolybdenum units. The strong interaction between the two $[\text{Mo}_2]$ units and the oxide bridge provides an extensive molecular overlap to distribute the unpaired electron over the metal centers and the linker.

TD-DFT calculations were also carried out on the tetranuclear compounds using the optimized geometry of the models $[\text{Mo}_2(\text{NHCHNH})_2]_2(\mu\text{-X})_2$ ($\text{X} = \text{OH}, \text{O}$). Such calculations have been useful in understanding the electronic spectra of compounds having two $[\text{Mo}_2]$ units linked by dicarboxylate groups.^{4f} On the basis of the calculations, the absorptions at about 449 nm for **1** are calculated at 470 nm for the two symmetry-allowed $\delta \rightarrow \delta^*$ -type transitions that are close in energy, namely HOMO-1 to LUMO+1 ($\delta - \delta \rightarrow \delta^* - \delta^*$) and HOMO to LUMO+2 ($\delta + \delta \rightarrow \delta^* + \delta^*$). For the oxide-bridged compound **2**, the relatively strong absorption at about 725 nm ($\epsilon = 2.1 \times 10^4 \text{ M}^{-1} \text{ cm}^{-1}$) is assigned to a HOMO-to-LUMO ($\delta - \delta \rightarrow \delta + \delta$) transition (calculated at 632 nm, $f = 0.2553$). The band, observed at 560 nm and calculated at 520 nm, is tentatively assigned to the HOMO-to-LUMO+1 ($\delta - \delta \rightarrow \delta^* - \delta^*$).

For the mixed-valence species **3**, the band at 722 nm is assigned to the transition of SOMO \rightarrow LUMO ($\delta - \delta \rightarrow \delta + \delta$) which is calculated at 782 nm. The band at 557 nm (calculated at 626) is a $\pi \rightarrow \delta$ transition. One electronic transition (HOMO-2 \rightarrow SOMO) is predicted in the NIR range, and the band appears experimentally in the electronic spectra at ca. $10\,400 \text{ cm}^{-1}$, as shown in Figure 2. This band is often referred to as a charge-transfer band.

Conclusion. A new mixed-valence compound, $[\text{Mo}_2(\text{DmCF}_3\text{F})_3(\mu\text{-O})_2\text{Mo}_2(\text{DmCF}_3\text{F})_3]\text{SbF}_6$ (**3**), which is the only one formally composed of two rare $[\text{Mo}_2^{5.5+}]$ units has been prepared and structurally characterized. The crystallographic results, NIR, and EPR data show this is an electronically

delocalized system, which is also consistent with the result from DFT calculations.

Experimental Section

Materials and Methods. Solvents were dried and then distilled under N_2 following conventional methods or purified under argon using a Glass Contour solvent purification system. The synthetic operations of **1** and **3** were conducted under N_2 using Schlenk line techniques. $\text{Mo}_2(\text{OAc})_4$ ¹⁷ and $\text{H}(\text{DmCF}_3\text{F})$ were prepared by following published methods;⁶ NOSbF_6 and a 0.5 M solution of NaOCH_3 in methanol, purchased from Aldrich, were used as received.

Physical Measurements. Elemental analyses were performed by Robertson Microлит Laboratories, Madison, NJ. ^1H and ^{19}F NMR spectra were recorded on a Mercury-300 NMR spectrometer with chemical shifts (ppm) referred to CDCl_3 and CFCl_3 , respectively. Electronic spectra in the UV–vis range were measured in the range of 200–800 nm on a Shimadzu UV-2501PC spectrophotometer. The NIR spectrum was obtained on a Bruker TEASOR 27 spectrometer. CVs and differential pulse voltammograms (DPVs) were collected on a CH Instruments electrochemical analyzer with Pt working and auxiliary electrodes, and Ag/AgCl reference electrode, using a scan rate of 100 mV s^{-1} (for CVs), and 0.1 M Bu_4NPF_6 (in CH_2Cl_2) as electrolyte. Under these experimental conditions, the $E_{1/2}$ ferrocenium/ferrocene (Fc^+/Fc) couple was measured at 440 mV. EPR spectra were recorded in solid state using a Bruker ESP300 spectrometer.

Preparation of $\text{Mo}_2(\text{DmCF}_3\text{F})_3(\mu\text{-OH})_2\text{Mo}_2(\text{DmCF}_3\text{F})_3$ (1**).** A 0.5 M solution of NaOCH_3 (30 mL) in methanol was added slowly to a mixture of yellow $\text{Mo}_2(\text{OAc})_4$ (430 mg, 1.00 mmol) and $\text{H}(\text{DmCF}_3\text{F})$ (1.00 g, 3.00 mmol) in 40 mL of THF. The reaction mixture was stirred for 2 h, leading to a red supernatant solution and white crystalline sodium acetate. After the solvent was removed under reduced pressure, the residue was extracted with 20 mL of CH_2Cl_2 . A mixture of isomeric hexanes (40 mL) was then added to the CH_2Cl_2 extract, followed by about 4 mL of H_2O . The mixture was stirred for 2 h, producing a yellow precipitate. The product was isolated by filtration, washed with $2 \times 20 \text{ mL}$ of ethanol, and then dried under vacuum. Single crystals formed by diffusing isomeric hexanes into a CH_2Cl_2 solution of **1**. Yield: 1.15 g, 46%. ^1H NMR (in CDCl_3 , ppm): 9.217 (s, 4H, $-\text{NCHN}-$), 8.125 (s, 2H, $-\text{NCHN}-$), 7.052 (d, 4H, aromatic C–H), 6.946 (d, 8H, aromatic C–H), 6.838 (m, 12H, aromatic C–H), 6.391 (d, 8H, aromatic C–H), 6.324 (d, 8H, aromatic C–H), 6.267 (d, 8H, aromatic C–H), 2.693 (s, 2H, $-\text{OH}$). ^{19}F NMR (in CDCl_3): 110.015 (s, 12 F, $-\text{CF}_3$), 109.604 (s, 24 F, $-\text{CF}_3$). UV–vis in CH_2Cl_2 , λ_{max} (nm) (ϵ , $\text{M}^{-1} \text{ cm}^{-1}$): 449 (4.2×10^3). Anal. Calcd for $\text{C}_{90.5}\text{H}_{57}\text{ClF}_{36}\text{N}_{12}\text{O}_2\text{Mo}_4$ (**1**·0.5 CH_2Cl_2): C, 44.41; H, 2.34; N, 6.87%. Found: C, 44.14; H, 2.10; N, 6.62%.

Preparation of $\text{Mo}_2(\text{DmCF}_3\text{F})_3(\mu\text{-O})_2\text{Mo}_2(\text{DmCF}_3\text{F})_3$ (2**).** A solution of **1** (480 mg, 0.200 mmol) in 20 mL of CH_2Cl_2 was stirred in air for 4 h, during which time the color of the solution gradually changed from yellow to green. The product was essentially quantitatively precipitated by addition of hexanes. Single crystals were obtained by evaporation in air of a CH_2Cl_2 and acetone solution of **2**. Yield: 0.42 g, 88%. ^1H NMR (in CDCl_3 , ppm): 9.372 (s, 2H, $-\text{NCHN}-$), 8.254 (s, 4H, $-\text{NCHN}-$), 7.076 (d, 4H, aromatic C–H), 6.993 (d, 4 H, aromatic C–H), 6.932 (d, 8 H, aromatic C–H), 6.767 (t, 8 H, aromatic C–H), 6.652 (d, 8H,

(17) Stephenson, T. A.; Bannister, E.; Wilkinson, G. *J. Chem. Soc.* **1964**, 2538.

Table 3. X-ray Crystallographic Data

compound	1·CH ₂ Cl ₂	2·H ₂ O	3·H ₂ O·CH ₂ Cl ₂
formula	C ₉₁ H ₅₈ Cl ₂ F ₃₆ Mo ₄ N ₁₂ O ₂	C ₉₀ H ₅₆ F ₃₆ Mo ₄ N ₁₂ O ₃	C ₉₁ H ₅₈ Cl ₂ F ₄₂ Mo ₄ N ₁₂ O ₃ Sb
fw	2490.15	2418.95	2740.07
space group	P1 (No. 2)	P2 ₁ /n (No. 14)	P1̄ (No. 2)
a (Å)	13.902(3)	25.102(6)	14.296(5)
b (Å)	14.435(3)	13.713(3)	15.033(5)
c (Å)	14.909(3)	28.118(7)	24.294(8)
α (deg)	64.168(3)	90	72.523(7)
β (deg)	79.495(3)	104.807(4)	86.086(7)
γ (deg)	62.515(3)	90	81.596(6)
V (Å ³)	2388.2(9)	9357(4)	4925(3)
Z	1	4	2
T (K)	213	213	213
d _{calcd} (g/cm ³)	1.731	1.714	1.848
μ (mm ⁻¹)	0.695	0.652	0.956
R1 ^a (wR2 ^b)	0.0663(0.1431)	0.0614(0.1148)	0.0933 (0.1632)

$${}^a R1 = \sum ||F_o| - |F_c|| / \sum |F_o|. \quad {}^b wR2 = [\sum [w(F_o^2 - F_c^2)^2] / \sum [w(F_o^2)^2]]^{1/2}.$$

aromatic C–H), 6.606 (d, 4H, aromatic C–H), 6.417 (d, 8H, aromatic C–H), 6.279 (d, 4H, aromatic C–H). ¹⁹F NMR (in CDCl₃, ppm): 109.928 (s, 12F, –CF₃), 109.755 (s, 24 F, –CF₃). IR (KBr, cm⁻¹): 1613 (w), 1591 (w), 1546 (s), 1491 (m), 1449 (m), 1324 (s), 1279 (w), 1212 (w), 1164 (m), 1125 (s), 1067 (m), 1000 (w), 973 (m), 898 (m), 885 (w), 793 (m), 756 (w), 696 (m), 656 (w). UV–vis in CH₂Cl₂, λ_{max} (nm) (ε, M⁻¹ cm⁻¹): 725 (2.1 × 10⁴), 560 (1.8 × 10³), 365 (sh), 281 (6.6 × 10⁴). Anal. Calcd for C₉₀H₅₄F₃₆N₁₂O₂Mo₄ (2): C, 44.98; H, 2.26; N, 6.99%. Found: C, 44.84; H, 1.94; N, 6.83%.

Preparation of [Mo₂(DmCF₃F)₃(μ-O)₂Mo₂(DmCF₃F)₃]SbF₆ (3). A mixture of 2 (240 mg, 0.100 mmol) and NOSbF₆ (26 mg, 0.10 mmol) in 15 mL of CH₂Cl₂ was stirred for 15 min and then was allowed to stand undisturbed overnight. The black crystalline product was isolated by filtration, washed with 2 × 10 mL of hexanes, and dried under vacuum. Yield: 71 mg, 27%. IR (KBr, cm⁻¹): 1616 (w), 1592 (w), 1542 (s), 1490 (m), 1449 (m), 1328 (s), 1278 (w), 1212 (w), 1174 (m), 1126 (s), 1069 (m), 977 (m), 893 (m), 798 (m), 756 (w), 696 (m), 653 (w). NIR (KBr, cm⁻¹): 10 400 (vs). UV–vis in acetone, λ_{max} (nm) (ε, M⁻¹ cm⁻¹): 722 (2.4 × 10⁴), 557 (2.1 × 10²), 365 (sh). Anal. Calcd for C₉₀H₅₆F₄₂N₁₂O₂Mo₄Sb (3·CH₂Cl₂): C, 40.13; H, 2.07; N, 6.17%. Found: C, 39.93; H, 1.72; N, 5.86%.

X-ray Structure Determinations. Single crystals suitable for X-ray analysis were mounted and centered on the tips of cryoloops attached to a goniometer head. Data for 1·CH₂Cl₂, 2·H₂O, and 3·H₂O·CH₂Cl₂ were collected at –60 °C on a BRUKER SMART 1000 CCD area detector system. Cell parameters were determined using the program SMART.¹⁸ Data reduction and integration were performed with the software package SAINT,¹⁹ while absorption corrections were applied using the program SADABS.²⁰ The positions of the heavy atoms were found via direct methods using the program SHELXTL.²¹ Subsequent cycles of least-squares refinement followed by difference Fourier syntheses revealed the positions of the remaining non-hydrogen atoms. Hydrogen atoms were added in idealized positions. Non-hydrogen atoms, except some atoms from disordered trifluoromethyl groups and solvent molecules, were refined with anisotropic displacement parameters.

(18) SMART V 5.05 Software for the CCD Detector System; Bruker Analytical X-ray System, Inc.: Madison, WI, 1998.

(19) SAINT. Data Reduction Software. V 6.36A.; Bruker Analytical X-ray System, Inc.: Madison, WI, 2002.

(20) SADABS. Bruker/Siemens Area Detector Absorption and Other Corrections. V2.03; Bruker Analytical X-ray System, Inc.: Madison, WI, 2002.

(21) Sheldrick, G. M. SHELXTL. V 6.12; Bruker Analytical X-ray Systems, Inc.: Madison, WI, 2000.

Crystallographic data for 1·CH₂Cl₂, 2·H₂O, and 3·H₂O·CH₂Cl₂ are given in Table 3, and selected bond distances and angles are given in Table 1.

Computational Details. DFT²² calculations were performed with the triplet Becke's²³ three-parameter exchange functional and the Lee–Yang–Parr²⁴ nonlocal correlation functional (B3LYP) in the Gaussian03 program.²⁵ Double-ζ quality basis sets (D95)²⁶ were used on C, N, and H atoms as implemented in Gaussian. Correlation consistent double-ζ basis sets (CC-PVDZ)²⁷ were applied for the O atoms. A small effective core potential (ECP) representing the 1s2s2p3s3p3d core was used for the molybdenum atoms along with its corresponding double-ζ basis set (LANL2DZ).²⁸ TD-DFT calculations²⁹ were performed to assign the electronic spectra of these compounds. All calculations were performed on either Origin 3800 64-processor SGI or Origin 2000 32-processor SGI supercomputers located at the Texas A&M supercomputing facility.

(22) (a) Hohenberg, P.; Kohn, W. *Phys. Rev.* **1964**, *136*, B864. (b) Parr, R. G.; Yang, W. *Density-Functional Theory of Atoms and Molecules*; Oxford University Press: Oxford, 1989.

(23) (a) Becke, A. D. *Phys. Rev. A* **1988**, *38*, 3098. (b) Becke, A. D. *J. Chem. Phys.* **1993**, *98*, 1372. (c) Becke, A. D. *J. Chem. Phys.* **1993**, *98*, 5648.

(24) Lee, C. T.; Yang, W. T.; Parr, R. G. *Phys. Rev. B* **1998**, *37*, 785.

(25) Frisch, M. J.; Trucks, G. W.; Schlegel, H. B.; Scuseria, G. E.; Robb, M. A.; Cheeseman, J. R.; Montgomery, J. A., Jr.; Vreven, T.; Kudin, K. N.; Burant, J. C.; Millam, J. M.; Iyengar, S. S.; Tomasi, J.; Barone, V.; Mennucci, B.; Cossi, M.; Scalmani, G.; Rega, N.; Petersson, G. A.; Nakatsuji, H.; Hada, M.; Ehara, M.; Toyota, K.; Fukuda, R.; Hasegawa, J.; Ishida, M.; Nakajima, T.; Honda, Y.; Kitao, O.; Nakai, H.; Klene, M.; Li, X.; Knox, J. E.; Hratchian, H. P.; Cross, J. B.; Bakken, V.; Adamo, C.; Jaramillo, J.; Gomperts, R.; Stratmann, R. E.; Yazyev, O.; Austin, A. J.; Cammi, R.; Pomelli, C.; Ochterski, J. W.; Ayala, P. Y.; Morokuma, K.; Voth, G. A.; Salvador, P.; Dannenberg, J. J.; Zakrzewski, V. G.; Dapprich, S.; Daniels, A. D.; Strain, M. C.; Farkas, O.; Malick, D. K.; Rabuck, A. D.; Raghavachari, K.; Foresman, J. B.; Ortiz, J. V.; Cui, Q.; Baboul, A. G.; Clifford, S.; Cioslowski, J.; Stefanov, B. B.; Liu, G.; Liashenko, A.; Piskorz, P.; Komaromi, I.; Martin, R. L.; Fox, D. J.; Keith, T.; Al-Laham, M. A.; Peng, C. Y.; Nanayakkara, A.; Challacombe, M.; Gill, P. M. W.; Johnson, B.; Chen, W.; Wong, M. W.; Gonzalez, C.; Pople, J. A. *Gaussian 03*, revision C.02; Gaussian, Inc.: Wallingford, CT, 2004.

(26) (a) Dunning, T. H.; Hay, P. J. In *Modern Theoretical Chemistry. 3. Methods of Electronic Structure Theory*; Schaefer, H. F., III, Ed.; Plenum Press: New York, 1977; pp 1–28. (b) Woon, D. E.; Dunning, T. H. *J. Chem. Phys.* **1993**, *98*, 1358.

(27) (a) Dunning, T. H. *J. Chem. Phys.* **1989**, *90*, 1007. (b) Woon, D. E.; Dunning, T. H. *J. Chem. Phys.* **1993**, *98*, 1358. (c) Wilson, A. K.; Woon, D. E.; Peterson, K. A.; Dunning, T. H. *J. Chem. Phys.* **1999**, *110*, 7667.

(28) (a) Wadt, W. R.; Hay, P. J. *J. Chem. Phys.* **1985**, *82*, 284. (b) Hay, P. J.; Wadt, W. R. *J. Chem. Phys.* **1985**, *82*, 299.

(29) Casida, M. E.; Jamorski, C.; Casida, K. C.; Salahub, D. R. *J. Chem. Phys.* **1998**, *108*, 4439.

Acknowledgment. We thank the Robert A. Welch Foundation and Texas A&M university for financial support. We are grateful to the Laboratory for Molecular Simulation at TAMU for hardware and software and the TAMU supercomputer facility.

Supporting Information Available: X-ray crystallographic data for **1**·CH₂Cl₂, **2**·H₂O, and **3**·H₂O·CH₂Cl₂ in standard CIF format. This material is available free of charge via the Internet at <http://pubs.acs.org>.

IC061352V